

Multiple Descents in Deep Learning as a Sequence of Order-Chaos Transitions

Wei Wenbo,¹ Nicholas Chong Jia Le,¹ Lai Choy Heng,¹ and Feng Ling^{2,1*}

¹*Department of Physics, National University of Singapore, 117551 Singapore and*

²*Systems Science Department, Institute of High Performance Computing, A*STAR, 138632 Singapore*

We observe a novel ‘multiple-descent’ phenomenon during the training process of LSTM, in which the test loss goes through long cycles of up and down trend multiple times after the model is overtrained. By carrying out asymptotic stability analysis of the models, we found that the cycles in test loss are closely associated with the phase transition process between order and chaos, and the local optimal epochs are consistently at the critical transition point between the two phases. More importantly, the global optimal epoch occurs at the first transition from order to chaos, where the ‘width’ of the ‘edge of chaos’ is the widest, allowing the best exploration of better weight configurations for learning.

I. INTRODUCTION

In deep learning, understanding the training dynamics has become paramount for enhancing model performance, generalization, and robustness. The training of deep neural networks involves navigating through complex, high-dimensional parameter spaces, where the interplay between model complexity, dataset characteristics, and learning algorithms dictates the learning trajectory. This process is far from straightforward, often characterized by phenomena such as overfitting, underfitting, and various forms of descent in performance metrics.

The dynamics of training deep neural networks are critical for several reasons. Generalization is a primary concern in machine learning, focusing on the model’s ability to generalize from training data to unseen data. Understanding how training dynamics affect generalization can lead to better strategies for model tuning [1, 2]. Optimization within deep networks is challenging due to the non-convex nature of loss landscapes, where insights into training dynamics inform the choice of optimizers, learning rates, and regularization techniques [3, 4]. Overfitting and underfitting are pivotal issues; the former occurs when a model memorizes training data too closely, while the latter happens when it fails to capture underlying patterns. Studying training dynamics aids in determining when to stop training to avoid these pitfalls [5, 6]. Lastly, dissecting the training process can enhance model interpretability by revealing which network parts are crucial for learning [7, 8].

The current understanding of training dynamics in deep learning involves several key concepts. The concept of the edge of stability posits that networks perform best when their parameters balance between order and chaos, optimizing learning capacity [9, 10]. The Neural Tangent Kernel (NTK) framework offers insights into how wide neural networks learn by resembling kernel methods in the infinite-width limit [11, 12]. Implicit regularization by optimization algorithms leads to better-than-

expected generalization [13, 14]. Exploring the loss landscape provides a visual understanding of how different optimization paths lead to minima with varied generalization capabilities [3, 15]. The scale of gradient noise during training correlates with model generalization, with higher noise often linked to better generalization [16, 17]. Lastly, normalization techniques like batch normalization have shown to stabilize learning and improve generalization [18, 19].

The double descent phenomenon has emerged as a significant area of study in recent years, particularly in the context of deep learning. Initially observed in classical statistics [20], this phenomenon describes a U-shaped curve in model performance where, after an initial decrease, the test error increases with model complexity or training duration before decreasing again. This behavior challenges the traditional understanding of the bias-variance trade-off and has been both empirically observed and theoretically analyzed in the context of neural networks [21, 22]. However, while double descent provides insights into how model complexity affects generalization, several open questions remain. These include the exact mechanisms behind why increasing model capacity can lead to better performance after an initial decline, the role of dataset size and noise, and how these observations extend to different types of architectures or learning tasks.

Our study introduces a novel observation of ‘multiple descents’ in the training of deep learning models, specifically in Long Short-Term Memory (LSTM) networks. We explore this through an extensive analysis of LSTM networks trained on the Large Movie Review Dataset for sentiment analysis. Our research reveals that during the training process, particularly in the overfitting phase, the test loss exhibits multiple cycles of increases followed by a sharp decline, a pattern not fully captured by existing models like double descent. And more importantly, the most optimal epoch is consistently at the first transition from order to chaos, where the ‘edge of chaos’ is the widest, allowing the best exploration of better weight configurations for learning.

One core contribution of this study is the identification of these cycles with specific phase transitions. We

* email: 0@criticality.ai

propose that each descent in test loss corresponds to a transition between order and chaos state during the evolution of the neural network from training, and the optimal performance is achieved at the edge of these transitions, particularly at the first such transition. By employing techniques from dynamical systems, specifically asymptotic stability analysis, we measure how perturbations in initial conditions propagate through the network, offering insights into when these order-chaos transitions occur.

We will detail the experimental setup where we over-train an LSTM model to observe these dynamics, provide some theoretical explanation why these transitions might occur, by drawing parallels with known behaviors in non-linear systems like the tanh map, and discuss the implications of these findings for training deep learning models, particularly in terms of finding optimal training epochs.

II. EXPERIMENT SETUP

We build a basic LSTM model to perform sentiment analysis of the Large Movie Review Dataset [23], which contains 50,000 labelled movie reviews from the Internet Movie Database (IMDb) and is a popular open-source dataset for natural language processing. The model is over-trained to 10000 epochs to induce overfitting in order to explore the rich order chaos transition behaviors. The embedding layer projects the individual words (tokens) into a learned continuous vector space, the LSTM layer performs the time-series analysis, and the output layer performs the final classification. The hyperparameters of the model are summarized in Table I.

We partition 70% of the dataset for training and 30% for testing, padding/truncating each review to a fixed length of 500 tokens. The model is optimized with the Adam optimizer with a learning rate of 0.0005.

A. Asymptotic stability analysis

We calculate the asymptotic trajectory separation/difference of the output recurrent unit of LSTM cell h_t under perturbation to extract the asymptotic stability of the LSTM model, specifically order and chaos phases. The key principle is the following: suppose we have a dynamic system (in this case the LSTM cell) with the

recurrence relation:

$$\mathbf{k}_t = \mathbf{F}(\mathbf{k}_{t-1}) \quad (1)$$

We add a small noise perturbation ε drawn from a Gaussian distribution at the 0th timestep to \mathbf{k}_0 , giving another input $\mathbf{k}'_0 = \mathbf{k}_0 + \varepsilon$. Iterating both \mathbf{k}_0 and \mathbf{k}'_0 for t steps (where t is large) gives two asymptotic values: \mathbf{k}_t and \mathbf{k}'_t . If the system is in an ordered state, the asymptotic distance

$$D = |\mathbf{k}'_t - \mathbf{k}_t| \quad (2)$$

converges to 0. Otherwise, they diverge, and it means the system is in the asymptotic chaos phase. Unlike the basic feedforward neural networks, the LSTM network has two different types of inputs. The first is an external input \mathbf{x}_t which corresponds to the input token at time step t , and the second is the recurrent input h_{t-1} from the previous time step.

To refresh, the following equations describe the different state vectors of an LSTM during a forward pass at timestep t :

$$\begin{aligned} \mathbf{i}_t &= \sigma(\mathbf{W}_{xi}\mathbf{x}_t + \mathbf{W}_{hi}\mathbf{h}_{t-1} + \mathbf{b}_i) \\ \mathbf{f}_t &= \sigma(\mathbf{W}_{xf}\mathbf{x}_t + \mathbf{W}_{hf}\mathbf{h}_{t-1} + \mathbf{b}_f) \\ \mathbf{o}_t &= \sigma(\mathbf{W}_{xo}\mathbf{x}_t + \mathbf{W}_{ho}\mathbf{h}_{t-1} + \mathbf{b}_o) \\ \tilde{\mathbf{c}}_t &= \tanh(\mathbf{W}_{xc}\mathbf{x}_t + \mathbf{W}_{hc}\mathbf{h}_{t-1} + \mathbf{b}_c) \\ \mathbf{c}_t &= \mathbf{f}_t \odot \mathbf{c}_{t-1} + \mathbf{i}_t \odot \tilde{\mathbf{c}}_t \\ \mathbf{h}_t &= \mathbf{o}_t \odot \tanh(\mathbf{c}_t) \end{aligned}$$

where \odot is the element-wise product, and σ is the sigmoid function $\frac{1}{1+e^{-x}}$.

The intrinsic order/chaos property of the network is to be characterized when there is no continuous external inputs or driving force to it. Therefore, the first 500 iterations of the LSTM are ignored for asymptotic analysis. After 500 iterations (input review length with padding), we let the LSTM continue running or iterating without external input values, i.e., $\mathbf{x}_t = 0$. To get the asymptotic distance, a noise perturbation is introduced to the output unit \mathbf{h}_{-1} , i.e., $\mathbf{h}'_{-1} = \mathbf{h}_{-1} + \epsilon$. Next, we evaluate the asymptotic trajectory difference between the original and perturbed output values of the LSTM cell, i.e., $|\mathbf{h}'_T - \mathbf{h}_T|$, with large T value at $T = 1599$.

B. Detailed method

Due to the high computational cost of our operation, we randomly sample only 500 reviews from the test dataset, which we then use across the rest of the experiments. This subset was used to keep our experiment consistent while being computationally tractable.

After each epoch during the training process, we obtain 500 asymptotic distances D from the 500 reviews, and then evaluate the average of their \ln values to extract the order/chaos state of the model at that epoch. Note

TABLE I: Structure of the model

Layer	Output Dimension
Embedding Layer	32
LSTM Layer	60
Fully Connected Layer	1

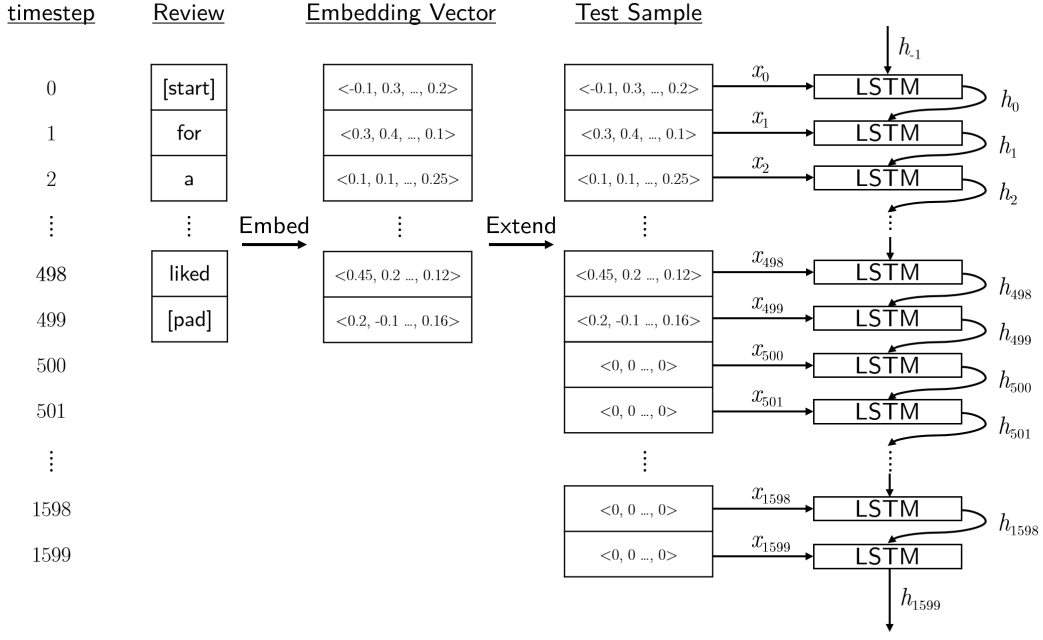


FIG. 1: Illustration of our methodology to iterate the LSTM cell to get the asymptotic value of output neuron h_T , where T is large at $T = 1599$. The first 500 iterations use words from the movie reviews as input, after which only **0** vectors are used as LSTM cell inputs to extract the order/chaos properties of the model.

that to account for machine precision in the numerical process, we add a tiny constant value $\exp(-15)$ to each asymptotic distance and use it as a reference to 0. This also means we regard $\ln D = -15$ to be the case where the model is in the ordered phase, as any value lower than may be due to machine precision and can be effectively treated as 0.

Fig. 1 demonstrates our main methodology for measuring the asymptotic distances. Our steps can be summarized as follows:

1. Pass a review from the test sample through the embedding layer to obtain $x_0 \dots x_{499}$, the embedding vectors from the real review. Extend the array of embedding vectors to 1600 time steps with the zero vectors $x_{500} \dots x_{1599}$.
2. At each timestep, propagate the review vector x_t along with the hidden vector h_{t-1} through the layer to the last timestep (in our case 1600) to obtain h_{1599} .
3. Repeat steps 1 and 2 with the same review, using an initial hidden vector $h'_{-1} = h_{-1} + \varepsilon$ (where ε is d -dimensional Gaussian noise), obtaining h'_{1599} .
4. Calculate the distance between h'_{1599} and h_{1599} , giving the asymptotic distance for the i -th review $D_i = |h'_{1599} - h_{1599}|$. Finally, add $\exp(-15)$ giving $D'_i = D_i + \exp(-15)$.
5. Repeat steps 1 to 4 for all 500 reviews in our test sample.

6. Calculate the \ln value of the geometric mean $\tilde{D} = \log \left(\sqrt[500]{D'_1 D'_2 \dots D'_{500}} \right)$, at this epoch for the 500 samples. We call \tilde{D} the ‘asymptotic distance’ for short.
7. Calculate the reduced sum $h_{1599} \cdot \mathbf{1}$ for each of the 500 reviews, where $\mathbf{1}$ is a vector of 1s, to visualize the bifurcation process to chaos of the model.
8. Repeat steps 1 to 7 for every epoch during model training, measuring \tilde{D} and $h_{1599} \cdot \mathbf{1}$ across the entire training process.

To reiterate, in step 6, if the asymptotic distance \tilde{D} is very negative (minimal value is -15 due to machine precision adjustment), it indicates the model is in the ordered phase. If it is significantly larger than -15 , it indicates the model is in the chaotic phase. To double check the order/chaos phase of the model, in step 7, the reduced sum $h_{1599} \cdot \mathbf{1}$ is calculated to project the high dimensional h_{1599} to 1 dimension to visualize the order/chaos states of the model. If the reduced sums of the 500 follow-up reviews converges to the same value, it indicates the model is in the ordered phase. If the reduced sums of the 500 reviews scatter, it indicates the model is in the chaotic phase.

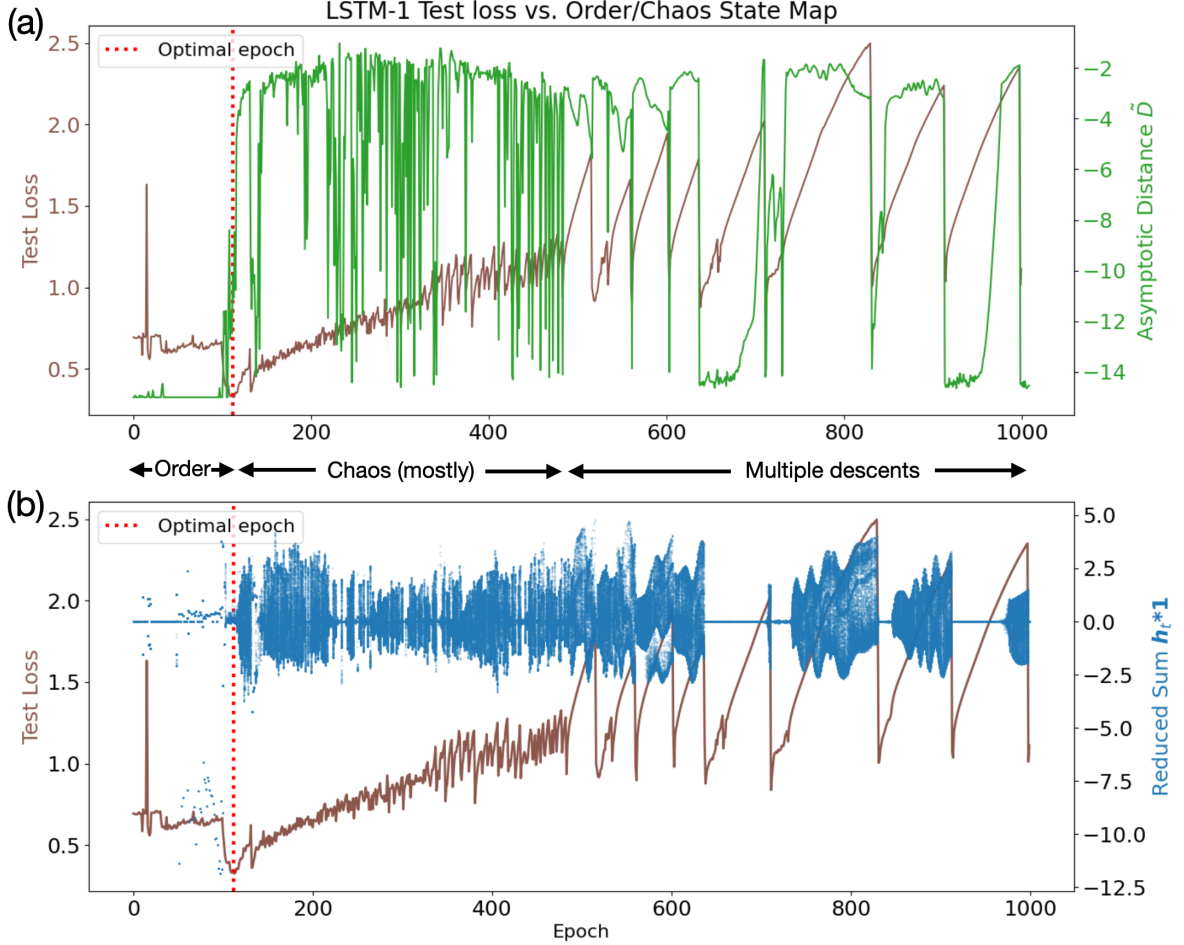


FIG. 2: Multiple descents through a sequence of order chaos transitions during the training process of LSTM. (a) The average asymptotic log distances \tilde{D} (green) under perturbation is used to indicate order/chaos states. The optimal epoch of lstm-1 is 114 with an accuracy of 88.34%. Multiple descents are seen in the overfitting regime at epochs > 450 . When the asymptotic distance is at -15 , it means two slightly different initial input values will converge to the same value at long enough iterations of the LSTM cell, indicating order phase. If the asymptotic distance is large, it means the model is at chaotic phase. (b) The ‘bifurcation map’ (blue) is shown together with the test loss (brown). The ‘bifurcation map’ is drawn by plotting the reduced sum $\mathbf{h}_{1599} \cdot \mathbf{1}$ for each of the 500 review samples at every epoch. Note that within every epoch, the average of all 500 reduced sums has been subtracted from each reduced sum value for the ease of visualization. Similarly, if the different samples converge to the same value, it indicates order phase. If the samples spread out, it indicates chaotic phase.

III. RESULTS ON MULTIPLE DESCENTS AND ORDER-CHAOS TRANSITIONS

By running the training process for 1000 epochs, we obtain two notable features.

First, when the model is overtrained and over-fitting happens after approximately 500 epochs, long cycles of test loss going up happen, and each cycle ends with a sudden and drastic drop within just one epoch. As seen in Fig. 2(a), 8 such cycles are clearly visible between epoch 500 and 1000. In each cycle, we can see the asymptotic distance of the model increases when test loss increases, and both quantities suffer from the same sudden and drastic drop near epochs like 600, 700, 850, and 1000

at the end of the cycle. This indicates that between epoch 500 and 1000, during each cycle the model performance gets worse as it becomes less stable (i.e., more chaotic), until suddenly the model performance gets better when it suddenly transitions from the chaotic phase to order phase. To even further demonstrate the order/chaos phases during the training process, we also plot the reduced sum $\mathbf{h}_{1599} \cdot \mathbf{1}$ for each of the 500 samples in every epoch in Fig. 2(b). We do this simple dimensionality reduction to 1 dimension to allow the ease of visualization. A detailed examination of the \mathbf{h}_{1599} vectors from different samples show that they are identical when their reduced sums are the same. Note that we have normalized the reduced sums by subtracting the average

over 500 samples in each epoch for better visualization, without affecting the conclusion of the results. In the epochs of order phase, the 500 samples converges to only one or several values, a typical feature of order phase; In the epochs of chaos phase, the 500 samples spread out vertically and do not converge.

Secondly, we can observe the first order to chaos transition occurs at epoch 114, when the model also achieves the lowest test loss throughout the whole training process. Such transition can be observed both in terms of the large asymptotic distance values after epoch 114 in Fig. 2(a), and the scattering of the 500 samples in Fig. 2(b). The same phenomenon has been observed in feedforward neural networks, that the ‘edge of chaos’ coincides with the optimal performance of the networks [24, 25]. However, our experiment here further indicates that although there are multiple descents with each associated with a transition between order and chaos during the training process; The best performance happens when the model enter from order to chaos for the first time.

Interestingly, such order chaos transition trends closely resemble that of a one-dimensional tanh map in dynamical systems, or rather the generic non-linear 1D map widely studied in dynamical systems, including the logistic map. The tanh map is an extension of the logistic map and is given by the following recurrence relation:

$$k_t = rk_{t-1}(1 - \tanh(k_{t-1})) \quad (3)$$

Since the LSTM equations contain mostly hyperbolic functions as non-linear activations, it is not surprising that LSTM exhibits a similar phase diagram as the tanh map. And indeed as seen from Fig. 3, the phase diagram of the tanh map also exhibits a first order chaos transition at $r \approx 9$, with many subsequent transitions after that. In LSTM during the training process, as we have not applied any regularization, the overall weight values keep increasing, effectively mimics the increasing value of r in the tanh map equation 3.

It is also widely observed that the first transition from order to chaos in non-linear dynamics like the tanh map and other non-linear maps is the slowest, as can be also seen in Fig. 3 the wide range of r values below 9. Our results indicate that LSTM has similar behavior, that the first entry from order to chaos is the slowest, followed by many (infinity) other order chaos transitions as the model weights (equivalent to r in the tanh map) increase overall with training. Since ‘edge of chaos’ is the best weights configuration for the model to process information [25], that means it is the easiest for the model to explore optimal configuration at the widest transition point, which is exactly the first order chaos transition around epoch 114 in Fig. 2. Therefore, the model is the most optimal at that epoch.

One clear evidence that the transition is the widest at the first order to chaos transition in LSTM is that we can observe a wide bifurcation regime in Fig. 2(b). From the beginning of training till around epoch 50, we see that

the reduced sum of the 500 samples mostly converge to only one unique value, which is typically known as the single fixed point in the order phase. Between epoch 50 and 100, the reduced sum ‘bifurcates’ into two values, before chaos kicks in. On the other hand, for the multiple descents regimes after epoch 450, the bifurcation of single fixed point value to multiple values is hardly visible, indication a very short bifurcation process from single fixed points to multiple points before transitioning to chaos. It is well-known that non-linear systems approach chaos exponentially fast at the same ratio of the Feigenbaum constant [26]. Therefore, the wider is the first bifurcation regime, generally the slower the system approaches chaos. That being said, the bifurcation process in high dimensional systems like LSTM may differ from that of the low dimensional tanh map or the logistic map, and more studies are needed to understand it better.

To ensure the reproducibility of the results, we have repeated the experiment with different random seeds, and the results consistently show the same phenomena of multiple descents and order chaos transitions. The most optimal epoch number may vary as seen in Appendixes Fig. 5, but it always coincides with the first order-to-chaos transition point. Additionally, the multiple descents are also always observed in the overfitting regime, with the locally optimal epoch (bottom of each loss cycle) coinciding with a transition between order and chaos. One thing to note is that, the order chaos transition during the multiple descents are not always drastic as in Fig. 2(a). As seen in Fig. 5, the asymptotic distances can have less drastic change at the locally optimal epoch than that in the first experiment shown in Fig. 2(a). But nevertheless, they are still clearly transitions since the sudden change in asymptotic distances occur within one epoch that coincides with the sharp drop in test loss. The less drastic changes near the bottom of the cycle (which is also order to chaos transition point) is likely due to one type of chaotic attractor to another, or the narrow order/chaos phase near the epoch as we illustrate in comparison with the well studied tanh map in Appendixes Fig. A. The detailed investigation of these transitions in the overfitting phase is beyond the scope of this work, but we will leave it for future studies.

IV. RELATIONSHIP BETWEEN TEST LOSS AND CHAOS DURING OVERFITTING

The multiple descents occur mainly in the overfitting regime in our experiments, or in other words after model has been well-trained. However, the large changes in loss function does not lead to similar changes in the model accuracy. This hints that while the model is less confident in its predictions as test loss decreases, it is not making significantly more incorrect predictions. Such phenomenon has been previously reported, that when overfitting, the increase in model loss can be attributed to an increase in loss on the incorrectly classified subset, rather

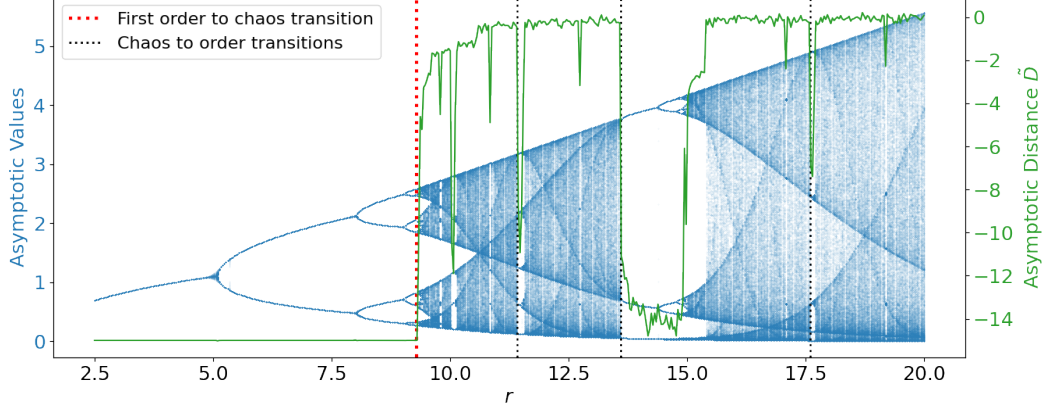


FIG. 3: The tanh bifurcation map in equation (3) showing the asymptotic distances (green) and the order/chaos (a.k.a. bifurcation) diagram (blue). 500 random initial values of k_0 are used.

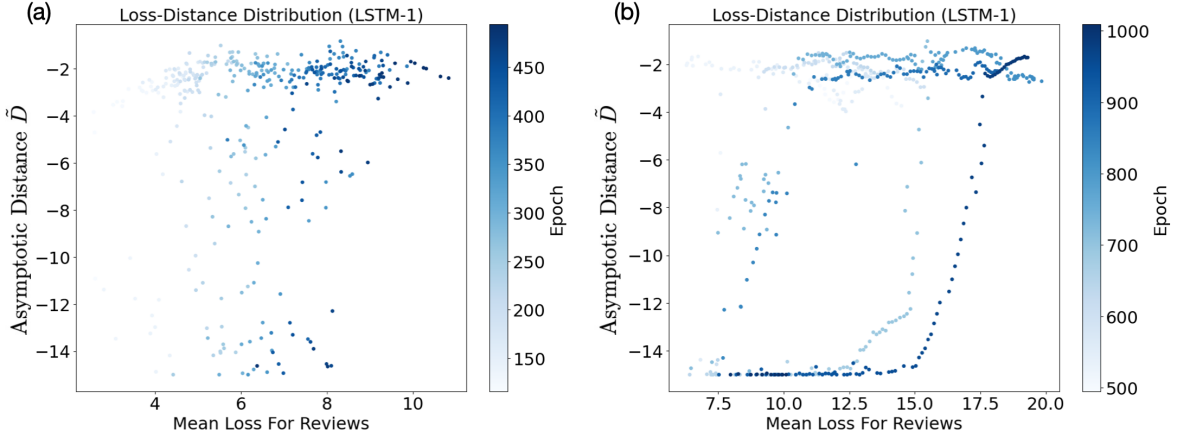


FIG. 4: Relationship between test loss of wrong predictions and chaos (as measured by asymptotic distance). (a) illustrates the overfitting regime before clear multiple descents happen, i.e., between epoch 115 and 495. (b) illustrates the region where clear multiple descents occur, i.e., after epoch 495.

than an increase in loss on the entire test set [27].

In our experiment from Section III, we used 500 reviews to generate the results for asymptotic distances. Here, we use the same reviews but focus specifically on those with incorrect model predictions which is approximately 75 samples (the exact value varies between epochs and models as the system experiences slight fluctuations in accuracy during the training process). The loss is then calculated only on this reduced subset of reviews.

Plotting the asymptotic distances against the loss on this subset (Fig. 4) reveals a clear relationship between these quantities during each descent cycle. In Fig. 4(b), we observe a clear correlation between loss and distance, with increasing loss generally relating to increased asymptotic distances. Furthermore, in Fig. 4(b), the distances increase rapidly together with the test loss, then reach a plateau. Such a plateau in distances is due to the fact that the activation functions in the LSTM satu-

rate, as they are hyperbolic activation functions. This is consistent with the behaviour of the tanh map in Fig. 3, where the system becomes less sensitive to changes in the input as it becomes very chaotic. Such a plateau does not mean the model is equally chaotic, as it can still reach the saturation distances at different rate. That is why the loss values still increases during this plateau. This is the same as the tanh map, where when the asymptotic distance reaches a plateau in Fig. 3, the Lyapunov exponent that characterize chaos actually increases.

Notice that before the multiple descents set in at epoch 495, as seen in Fig. 4(a), even if the model overfits after epoch 114, the monotonic relationship between test loss and chaos is not clear. This is likely because the model is mostly in the chaotic phase and the asymptotic distances are easily saturated. This can be seen in Fig. 2(b), where the 500 samples have a large dispersion between epoch 115 and 495 in most of the time, indi-

cating that the model is mostly chaotic. One thing to note between epoch 114 and 495 is that, there are narrow regimes of order phase in between this wide and mostly chaotic regime. This can be seen from Fig. 2(a) when the asymptotic distances are around -15, and also from Fig. 2(b) when the reduced sum of the 500 samples converge to one unique value, both very briefly. The order phases are so narrow, that on the whole scale of things the associated changes in test loss appears as noise. But in actual fact, they are intermittent order phases that are associated with the local minima in the loss function. Similar narrow gaps of order can also be seen in the tanh map in Fig. 3, and it has been well established in non-linear dynamics that these order phases after the first transition to chaos arrives from period-doubling bifurcation of prime-numbered periodic cycles [28].

V. RELATED WORK

In the landscape of deep learning research, our study discovers a strong link between loss fluctuations and the stability of the model, providing a new aspect of training dynamics. Past studies have delved into phenomena like double descent [20, 21], where performance metrics follow a U-shaped curve with respect to model complexity or training duration. Similarly, epoch-wise performance variations have been noted, suggesting that beyond model size, the training process itself can exhibit complex behaviors [1, 21]. However, our research advances this understanding by introducing the concept of multiple descents, where the test loss in LSTM networks undergoes repeated cycles of increases and sharp decreases, particularly in the overfitting phase. This observation diverges from the controlled oscillation of performance through cyclic learning rates as proposed by [29], or the exploration of stability edges by [9], who discuss the benefits of training at the brink of stability for optimal learning. There are many other studies that are also related, but we are not able to cover all of them here.

VI. DISCUSSION

In this work, we discovered a novel feature of ‘multiple descents’ during the training process of a deep learning

model. Our findings notably link these multiple descents to the intrinsic dynamical transitions between order and chaos within the network. By leveraging asymptotic stability analysis, akin to the approaches proposed by [25] to explore optimal machine intelligence at the edge of chaos. However, unlike their work which deems the asymptotic edge of chaos as the optimal model configurations, we find that only the first edge of chaos is the most optimal, whereas the others are simply local optimal. This provides a new theoretical perspective on when and why neural networks achieve peak performance, differing from previous studies which might focus on model size, dataset characteristics, or learning rate adjustments [3, 22, 29]. Our work not only extends the theoretical framework beyond the traditional bias-variance trade-off but also offers practical implications for model training, suggesting new strategies for training models at optimal epochs and potentially enhancing model generalization by understanding and navigating these chaotic dynamics with more principles. This could lead to more robust deep learning models, especially in scenarios where traditional overfitting mitigation strategies fall short [6, 13].

One particular remarkable finding of our work is that, despite its high dimensions, the LSTM training process exhibits a similar phase diagram structure as the well-known tanh map in dynamical systems, that the systems goes through bifurcation process to chaos, with the first order chaos transition being the widest, followed by many narrower regimes of order phases. Given the generic nature of this bifurcation diagram structure across different non-linear dynamics other than hyperbolic functions, it is likely that the qualitative patterns in our findings are not unique to LSTM, but can be generalized to other deep learning models. This opens up a new avenue of research in understanding the training dynamics of deep learning models, leveraging on the established theories in non-linear dynamical systems, and potentially lead to new training strategies that can improve the generalization and robustness of the model. That being said, more in-depth theoretical studies are needed to understand the exact reason behind the similarities between LSTM and the tanh map, and to explore the generalizability of our findings to other deep learning models.

-
- [1] M. Geiger, A. Jacot, S. Spigler, F. Gabriel, L. Sagun, S. d’Ascoli, G. Biroli, C. Hongler, and M. Wyart, *Journal of Statistical Mechanics: Theory and Experiment* **2020**, 023401 (2020).
 - [2] C. Zhang, S. Bengio, M. Hardt, B. Recht, and O. Vinyals, *Communications of the ACM* **64**, 107 (2021).
 - [3] H. Li, Z. Xu, and W. E, arXiv preprint arXiv:1804.08875 (2018).
 - [4] S. J. Reddi, S. Kale, and S. Kumar, arXiv preprint arXiv:1904.09237 (2018).
 - [5] N. Srivastava, G. Hinton, A. Krizhevsky, I. Sutskever, and R. Salakhutdinov, *Journal of Machine Learning Research* **15**, 1929 (2014).
 - [6] I. Goodfellow, Y. Bengio, and A. Courville, *Deep Learning* (MIT Press, 2016).
 - [7] M. D. Zeiler and R. Fergus, *European conference on computer vision*, 818 (2014).
 - [8] C. Olah, A. Mordvintsev, and L. Schubert, *Distill* (2017).

- [9] J. Cohen, A. Shashua, and O. Shamir, arXiv preprint arXiv:2103.00065 (2021).
- [10] S. Arora, J. Cohen, and E. Hazan, arXiv preprint arXiv:1802.06509 (2018).
- [11] A. Jacot, F. Gabriel, and C. Hongler, arXiv preprint arXiv:1806.07572 (2018).
- [12] J. Lee, L. Xiao, S. S. Schoenholz, Y. Bahri, J. Sohl-Dickstein, and J. Pennington, Advances in Neural Information Processing Systems (2019).
- [13] B. Neyshabur, S. Bhojanapalli, D. McAllester, and N. Srebro, Advances in Neural Information Processing Systems **30** (2017).
- [14] S. Gunasekar, J. D. Lee, D. Soudry, and N. Srebro, Advances in Neural Information Processing Systems (2018).
- [15] T. Garipov, P. Izmailov, D. Podoprikin, D. Vetrov, and A. G. Wilson, Advances in Neural Information Processing Systems (2018).
- [16] S. L. Smith, P.-J. Kindermans, C. Ying, and Q. V. Le, arXiv preprint arXiv:1711.00489 (2018).
- [17] N. S. Keskar, D. Mudigere, J. Nocedal, M. Smelyanskiy, and P. T. P. Tang, arXiv preprint arXiv:1609.04836 (2017).
- [18] S. Ioffe and C. Szegedy, arXiv preprint arXiv:1502.03167 (2015).
- [19] S. Santurkar, D. Tsipras, A. Ilyas, and A. Madry, Advances in Neural Information Processing Systems (2018).
- [20] M. Belkin, D. Hsu, S. Ma, and S. Mandal, Proceedings of the National Academy of Sciences **116**, 15849 (2019).
- [21] P. Nakkiran, G. Kaplun, Y. Bansal, T. Yang, B. Barak, and I. Sutskever, Journal of Statistical Mechanics: Theory and Experiment **2021**, 124003 (2021).
- [22] S. Mei and A. Montanari, Communications on Pure and Applied Mathematics **75**, 667 (2022).
- [23] A. L. Maas, R. E. Daly, P. T. Pham, D. Huang, A. Y. Ng, and C. Potts, in *Proceedings of the 49th Annual Meeting of the Association for Computational Linguistics: Human Language Technologies* (Association for Computational Linguistics, Portland, Oregon, USA, 2011) pp. 142–150.
- [24] L. Zhang, L. Feng, K. Chen, and C. H. Lai, International Journal of Artificial Intelligence and Robotics Research **1**, 2350001 (2024).
- [25] L. Feng, L. Zhang, and C. H. Lai, arXiv preprint arXiv:1909.05176 (2019).
- [26] M. J. Feigenbaum, Los Alamos Theoretical Division Annual Report **1976**, 1976 (1975).
- [27] S. Salman and X. Liu, arXiv preprint arXiv:1901.06566 (2019).
- [28] E. Sander and J. A. Yorke, Ergodic theory and dynamical systems **31**, 1249 (2011).
- [29] L. N. Smith, 2017 IEEE Winter Conference on Applications of Computer Vision (WACV), 464 (2017).

Appendix A: Additional LSTM models

Fig. 5 shows two other experiments that have slightly different look from results in Fig. 2(a), with different random seeds. Note that we use the model in the main text because these two experiments have slightly worse performance in terms of best test accuracy than the model presented in the main text. Unlike in Fig. 2, the asymptotic distances in Fig. 4 do not drop to 0 (or -15 in our case) at the end of each cycle, but to moderate values around -8 . This is likely due to the fact that the order/chaos transition is very narrow around the locally optimal epoch, and the resolution of our sampling (1 epoch) is not enough to capture the full picture of the order chaos transition. In other words, the order chaos transitions still exist, but they lie between two adjacent epochs. Since our measurements do not afford resolution higher than every epoch, this misses the exact transition point where the asymptotic distances should be 0.

This is further illustrated in Fig. 6 on the tanh map, which we previously drew analogy to. In high resolution map Fig. 6(b) with 281 different r values, we can clearly see a very narrow regime of order phase around $r = 10.675$, where the asymptotic distance drops drastically. However, in the low resolution map Fig. 6(a) with only 50 different r values, the order phase is not captured, and the asymptotic distance stays high at $r = 10.675$.

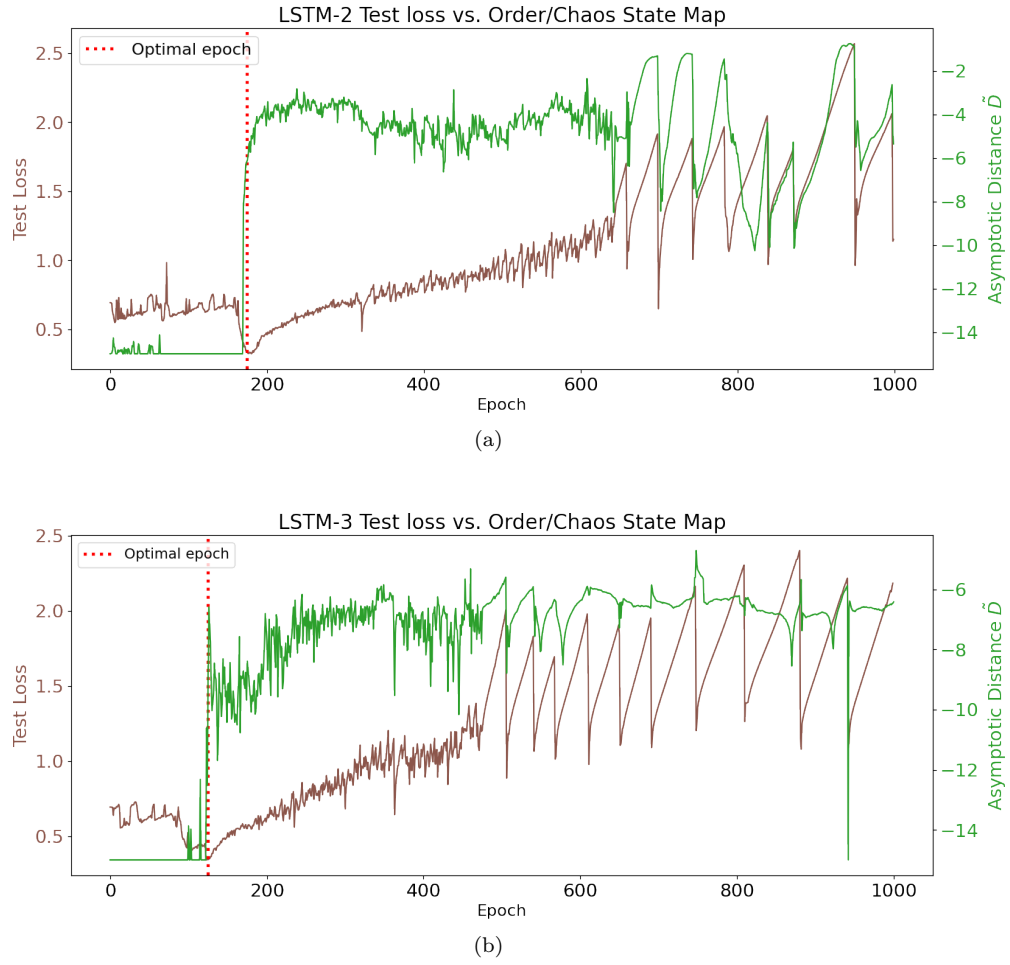


FIG. 5: Two other experiments with the same setting showing multiple descents, and best epoch occurring at the first order to chaos transition at (a) epoch 190 and (b) epoch 120.

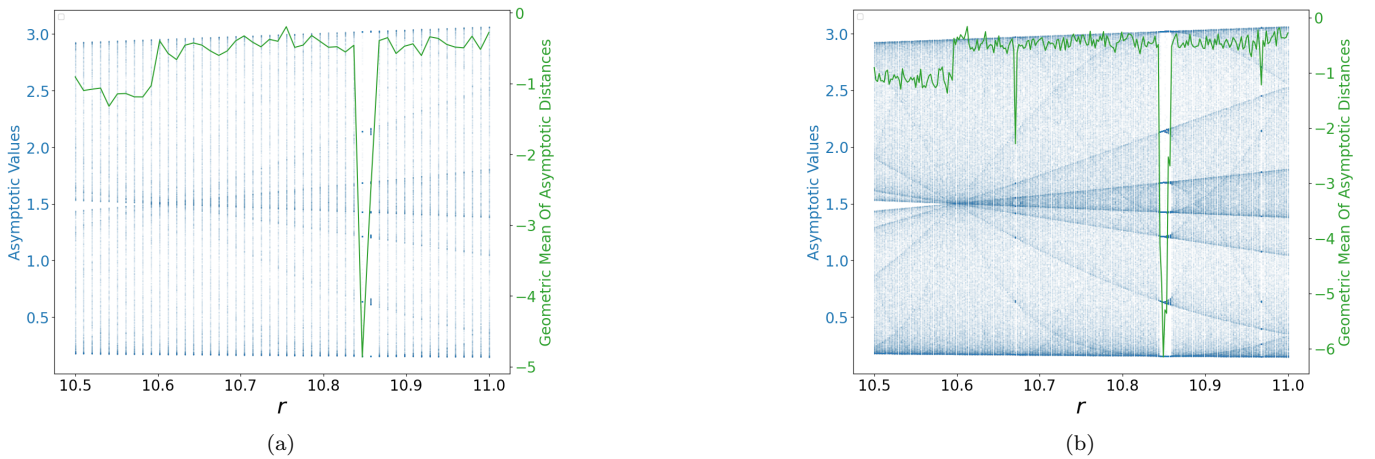


FIG. 6: tanh map plotted at two different sampling resolutions, with r ranging from 10.5 to 11. The low resolution map (a) covers 50 different values of r , while the high resolution map (b) covers 281 different values of r . The high resolution map (b) clearly shows the transitions to order at $r = 10.675$ due to the presence of an order phase, while the low resolution map (a) misses this transition.